applied sciences

MDPI

Article

Impact of Tungsten on Thermomechanically Induced Precipitation of Laves Phase in High Performance Ferritic (HiperFer) Stainless Steels

Jana Pöpperlová [1,*], Xiuru Fan [2], Bernd Kuhn [2], Wolfgang Bleck [1] and Ulrich Krupp [1]

[1] Steel Institute RWTH Aachen University (IEHK), Intzestr. 1, 52072 Aachen, Germany; bleck@iehk.rwth-aachen.de (W.B.); Krupp@iehk.rwth-aachen.de (U.K.)

[2] Institute of Energy and Climate Research (IEK), Microstructure and Properties of Materials (IEK-2), Forschungszentrum Jülich GmbH, 52425 Jülich, Germany; x.fan@fz-juelich.de (X.F.); b.kuhn@fz-juelich.de (B.K.)

* Correspondence: Jana.Poepperlova@iehk.rwth-aachen.de; Tel.: +49-241-80-95786

Received: 9 June 2020; Accepted: 24 June 2020; Published: 28 June 2020



Abstract: High-chromium ferritic stainless steels strengthened by Laves phase precipitates were developed for a high-temperature application in steam power plants. The impact of tungsten content on the precipitation of the intermetallic Laves phase during the newly developed thermomechanical process route was investigated. Due to rapid thermomechanically induced precipitation, a considerable reduction in processing time in comparison to the conventional solely thermal two-step processing of high chromium ferritic steels was achieved. Nevertheless, comparable mechanical properties at room temperature, i.e., the ultimate tensile strength of 712 MPa and the yield strength of 434 MPa, were obtained. The microstructure was analyzed by scanning electron microscopy (SEM) in combination with digital particle analysis, to estimate the particle size and the phase fraction of the Laves phase. The mean particle size of 52 nm and the volume fraction of 4.11% were achieved. Due to the tungsten content, an increase in the volume fraction and particle size was observed, giving rise to the higher strengthening effect.

Keywords: high chromium ferritic steel; intermetallic phase; Laves phase; precipitation; thermomechanical treatment

1. Motivation and Introduction

In recent years, environmental restrictions on CO_2 emission have demanded advanced power plants with higher efficiency. For further efficiency improvement, an increase of steam conditions to approximately 650 °C (300 bar) would be required. The present study is part of a project that aims to develop high-chromium fully ferritic stainless steels for application in ultra-super-critical power plants, with an operation temperature of 650 °C. The goal of this project was to achieve a stable ferritic, heat-resistant microstructure by combining solid solution and Laves phase precipitation strengthening.

The steels currently used in power plants provide certain disadvantages with respect to the high operation temperature of 650 °C. The conventional alloy concept of the 9 wt. % chromium ferritic-martensitic steels is challenged regarding the required steam oxidation resistance. These steels are below the limit for forming protective chromium oxide layers in steam at a temperature range of 550 to 650 °C due to their low chromium content [1]. As a result, their resistance to steam oxidation shows high fluctuation ranges and depends on many parameters, which means great uncertainty for stable use [1–3]. For example, the application of the common ferritic-martensitic steel P92 is limited to a maximum operation temperature of 620 °C due to the restricted thermodynamic stability of the strengthening precipitates in combination with the limited steam oxidation resistance [4]. Chromium

contents higher than 15 wt. % are necessary to reliably reduce steam oxidation at 650 °C [5]. In general, the creep resistance of ferritic-martensitic steels is based on microstructural stabilization by finely precipitated carbides and nitrides [6]. However, due to the higher chromium content (11–12 wt. %), ferritic-martensitic steels tend to the precipitation of Z-phase (Cr(V,Nb)N), which replaces nitrides as a more thermodynamically stable phase and therefore causes a reduction in creep resistance during long term operation [7,8]. An improvement in the creep resistance of ferritic-martensitic steels has been achieved with higher chromium contents of up to 14 wt. % in combination with controlled precipitation of the intermetallic Laves phase [9]. The formation of the Z-phase has not been observed in these steels. Furthermore, it has been attempted to use the Z-phase for strengthening [10,11]. Consequently, the maximum operation temperature of all currently available ferritic-martensitic steels is about 610 to 630 °C [4,12,13]. The maximum chromium content of ferritic-martensitic steels is controlled by the availability of a high-temperature austenitic phase field, which is about 14 wt. % Cr if a martensitic microstructure has to be achieved [14]. In most cases this value is even lower due to the avoidance of the undesirable δ-ferrite formation during solidification. Considering the low chromium content and the resulting limited steam oxidation resistance, the concept of high-temperature ferritic-martensitic steels appears to be exhausted for the current required highly efficient power plants.

Full ferritic steels with a higher chromium content than 15 wt. %, without martensitic transformation and strengthened by Laves phase precipitation, provide potentially sufficient steam oxidation resistance of up to 650 °C [5]. The main task of alloy design is to maximize the volume fraction of the strengthening Laves phase and to avoid the formation of the brittle σ-phase. A high chromium content of over 15 wt. % provides in principle a sufficient steam oxidation resistance of up to 650 °C [15]. However, the intermetallic Laves phase precipitation binds chromium from the matrix, which reduces the chromium fraction in solid solution to only 12.5 wt. % [16]. Therefore, a potential improvement of the steam oxidation resistance can only be expected if the Cr-content is significantly increased. A group of 22 wt. % steels (Crofer® 22) were originally developed for applications in high temperature fuel cell stacks [17]. Due to the addition of the alloying elements W, Nb, and Si, a favorable combination of creep strength and steam oxidation resistance is provided [17,18]. This strengthening effect is achieved by the precipitation of the intermetallic $(Fe,Si,Cr)_2(W,Nb)$ Laves phase at the grain boundaries as well as inside the grain [19]. In addition to the Laves phase, the formation of the undesirable brittle σ-phase (Fe,Cr) is characteristic of high-chromium steels. The reduction of the Cr-content to 17–18 wt. % leads to a required suppression of the σ-phase formation in the operation temperature range from 620 to 650 °C [19]. Simultaneously, this Cr-content of 17–18 wt. % is sufficient to improve steam oxidation resistance even after the precipitating of the Laves phase. The increased contents of W (3.6 wt. %) and of Nb (1.0 wt. %) for further improved mechanical properties, especially thermomechanical fatigue resistance, make the Fe17Cr2.6W and Fe17Cr3.6W steel designed in this work a competitor even for austenitic steel grades [20].

The present work focusses on the deformation-induced precipitation of the Laves phase as part of a new developed thermomechanical processing route and deals with the impact of tungsten on the precipitation behavior. The new thermomechanical processing route uses the rapidly occurring precipitation of the Laves phase during a hot deformation process. This enables a significantly shortened process route because hot forming, heat treatment and precipitation annealing are integrated in a one-step process. Consequently, the conventional two-step tempering, taking hours to precipitate Laves phase particles, can be shortened, resulting in precipitation within minutes. The conventional thermal process route as well as the developed "integrated" thermomechanical process route are schematically shown in Figure 1. The conventional tempering treatment for Laves phase precipitation consists of two separate steps. The first step at 520–550 °C serves to nucleate the particles. The desired growth and coarsening of the particles are provided by the second tempering step at 60–650 °C. The integrated thermomechanical process contains two deformation steps (forging I and forging II). Forging I represents a partial deformation followed by recrystallization. The final one-step deformation, forging II, guarantees the precipitation. The present work specifically deals with the final deformation for

Laves phase precipitation (forging II). The alloying element tungsten represents the strongest Laves phase-forming element in the high chromium Laves phase-strengthened stainless steels.

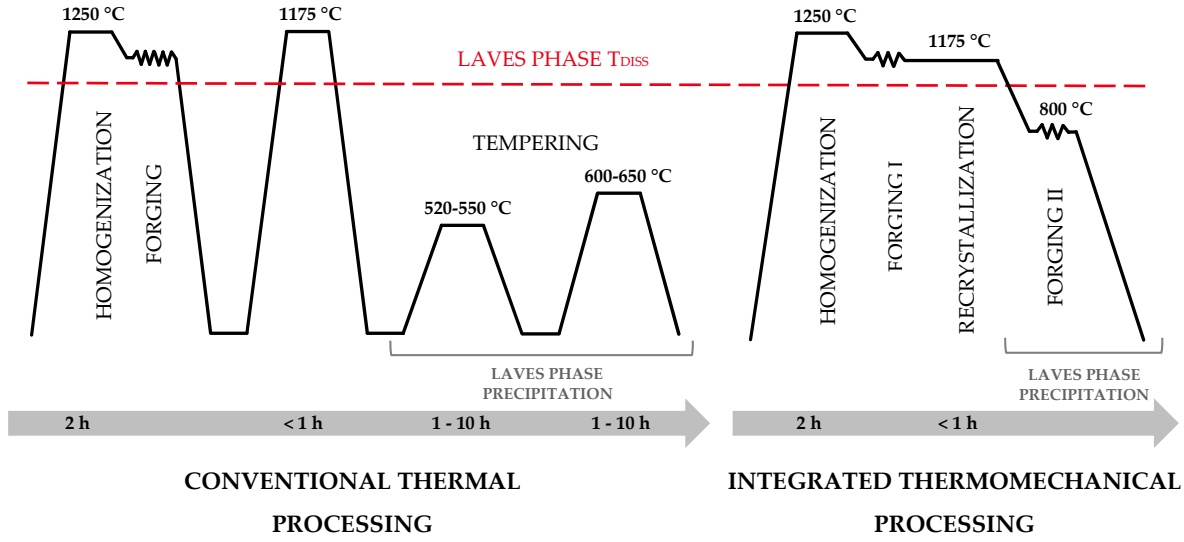


Figure 1. Conventional thermal versus integrated thermomechanical process routes with indicated Laves phase dissolution temperature T_{DISS}.

2. Experimental Procedure

2.1. Alloy Modelling and Manufacturing

The tested alloys were designed by using the thermodynamic modelling software TermoCalc®, which is based on the CALPHAD method [21]. This software tool was used for calculating the phase equilibria, evaluating the amount and stability of the phase constituents, and additionally for the determination of the impact of the main alloying elements. All presented calculations were performed using the nominal chemical composition of 17 wt. % Cr, 0.2 wt. % Mn, 0.25 wt. % Si, 1 wt. % Nb, and a variation in W, utilizing the TCS steel database TCFE8 [22].

The high purity model alloys Fe17Cr2.6W and Fe17Cr3.6W, which are tested in the present work, were manufactured by 2 kHz vacuum induction melting. The approximately 80 kg ingots ($140 \times 140 \times 535$ mm^3) were hot-forged after homogenization treatment utilizing a 400 t hydraulic press in three steps to a cross-section of 92×92 mm^2.

2.2. Thermomechanical Treatment

To investigate the influence of tungsten on thermomechanically induced Laves phase precipitation and its impact on mechanical properties, experiments were performed with the thermomechanical treatment simulator (TTS) at Steel Institute IEHK. The TTS facility enables the experimental simulation of industrial forging processes on a laboratory scale. The specimen, with a size of $15 \times 15 \times 65$ mm^3, was placed in the TTS test chamber, shown in Figure 2. The test chamber was evacuated and flooded with an inert gas; the temperature was measured and controlled using Pt10Rh-Pt thermocouples welded onto the sample. The specimen was inductively heated up with a water-cooled copper coil to a dissolution annealing temperature of 1200 °C with a heating rate of 100 °C·min^{-1} and held at this temperature for 40 min. The dissolution annealing serves to achieve a precipitation-free ferritic microstructure prior to the deformation process. After the dissolution annealing the specimen was cooled down to the deformation temperature of 800 °C with a cooling rate of 50 °C·s^{-1}. The cooling was accomplished by four gas nozzles blowing argon or helium for quenching onto the sample. The deformation process was performed in one step with a deformation grade of 0.5 by laterally arranged tungsten stamps. Subsequently, the deformed sample was isothermally tempered at the

deformation temperature of 800 °C for 60 s and finally quenched with a quenching rate of 150 °C·s^{-1}. The chosen deformation parameters were determined based on previous experiments. From the deformed TTS, sample secondary specimens could be prepared for tensile, compression or Charpy impact tests.

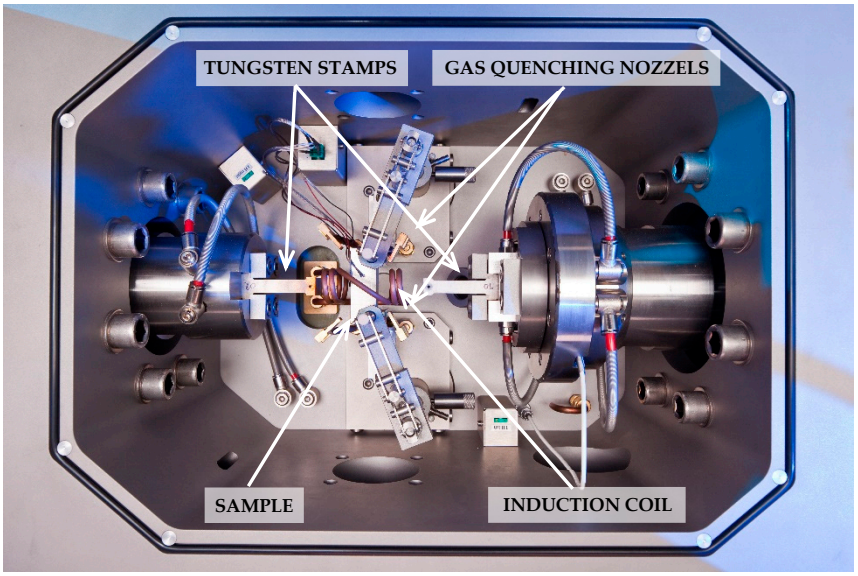


Figure 2. Test chamber of the Thermomechanical Treatment Simulator TTS 820.

2.3. Mechanical Testing

Tensile tests were performed to observe the impact of varying tungsten content, the main Laves phase forming element, on the strengthening effect of the precipitated Laves phase particles and their phase fraction. For the mechanical testing, the treated TTS samples were machine-cut into corresponding small sized tensile test specimens $10 \times 2 \times 1$ mm^3. The tensile tests were performed at room temperature utilizing an Instron 8862 universal testing machine.

2.4. Microstructural Investigation

After the forging process, the microstructure was characterized by means of scanning electron microscopy (SEM) in combination with energy dispersive X-ray spectroscopy (SEM-EDX). The investigations were carried out on polished samples using the Zeiss Σigma SEM equipped with an inlens detector for high-resolution SEM imaging and the Oxford X-Max 50 silicon drift EDX detector. The digital image analysis software AnalysisPro® supported the quantitative investigation of the microstructure. The standard post-processing of SEM micrographs before analysis includes filtering, shading correction, and contrast and intensity optimization to reduce statistical interference and improve the image quality. The post-processed SEM micrographs were then binarized and subsequently analyzed. The particle analysis utilizing AnalysisPro® was based on the calculated particle equivalent circle diameter (ECD), which is a diameter of a circle whose projection surface is identical to that of the particle. All data on the particle size refer to the precipitates in the grain interior, since the precipitates at the grain boundaries are too close to each other for differentiation between individual particles to be distinct or possible. Due to the limited resolution of the original SEM micrographs, all precipitates below 10 nm diameter were excluded from the evaluation. The identified larger components—for instance, niobium oxides—were also not considered to be relevant for the particle analysis. The Laves phase fraction was evaluated as a percentage area fraction of the precipitates only in the grain interior without considering the particle-free zones (PFZ), which typically develop along high angle grain boundaries [23]. This applied method is in accordance with the particle analysis procedure reported in [24,25].

3. Results and Discussion

3.1. Alloy Design

The alloy concept of fully ferritic stainless steels strengthened by the Laves phase focuses on high creep strength and steam oxidation resistance. The design is based on experience from the development of the commercial-grade Crofer® 22 H [17,18] and on the previous development of ferritic 17 wt. % Cr steels at IEK-2 [19,20,26]. The chemical composition of the experimental melting was developed by systematically varying the concentration of the mean alloying, Laves phase-forming elements. Thermo-Calc® calculations (utilizing the TCFE8 database) were performed for the reduced chromium content concept of 17 wt. % to accomplish the stability reduction of the embrittling σ-phase. The aim of the design was to maximize the volume of the Laves phase at the operating temperature (650 °C).

The presence of carbides in ferritic steels limits the creep strength, due to their size and tendency to coarsen further. As a result, the formation of additional finer precipitate is suppressed [15,19]. The intermetallic phase particles exhibit less tendency toward coarsening compared to the carbides; therefore, they significantly improve the creep strength [27]. The objective of optimization is to minimize losses of the Laves-phase-forming alloying elements tungsten and niobium due to the undesired formation of carbide, nitride, and carbonitride phases. In order to avoid this formation, the contents of carbon, nitrogen, and titanium are kept low [18,19]. Alloying silicon during production for the deoxidation of the melt positively influences the precipitation kinetics of the Laves phase, accelerating its formation by decreasing the solubility of tungsten in the matrix [27,28]. Additionally, the silicon itself is incorporated into the Laves phase precipitates [29].

According to the thermodynamic calculations, the combined addition of the alloying elements W, Nb and Si leads to the ferritic structure shown in Figure 3. This thermodynamic calculation was performed with the nominal chemical composition. The phase diagram predicts that the reduced chromium content implies a suppressed σ-phase stability under 620 °C as required. Two different Laves phases are present, denoted as the low-temperature Laves phase (LT Laves phase) and the high-temperature Laves phase (HT Laves phase) depending on their temperature range of stability. Tungsten and niobium show low solubility in ferrite; therefore, they extend the stable ferrite area and improve the stability of the precipitates. Due to their large atomic radii, these alloying elements contribute significantly to strengthening the solid solution. Tungsten, as the main Laves phase-forming element in this steel class, serves in general as the stimulator and stabilizer of the precipitates. The phase diagram shows the stability ranges of the respective phases as a function of the temperature and tungsten content. An increasing tungsten content slightly increases the stability of the HT Laves phase and the σ-phase. Maximum stability of the LT Laves phase is reached at 737 °C with a tungsten content of 2.3 wt. %. The target operating temperature of 650 °C is indicated by the red line and defines the relevant interval of 1.0 to 3.7 wt. % tungsten, in which the two Laves phases occur together.

Based on the calculation shown in Figure 4, the Laves phases exhibit the same crystal structure (hexagonal C14). However, they are lightly differentiated in chemical composition. The LT Laves phase $(Fe,Cr,Si)_2(Nb,W)$ exhibits higher niobium content, while the HT Laves phase $(Fe,Cr,Si)_2(W,Nb)$ contains more tungsten. Corresponding to the chemical composition of both Laves phases and based on the higher niobium diffusivity in the ferritic matrix, a metastable nature is expected of the LT Laves phase. The metastable nature implies specific mechanisms of the formation and change of chemical composition of the LT Laves phase into the final stable HT Laves phase [24,30]. In general, consecutive Laves phase tungsten enrichment during annealing has been reported [24,31,32].

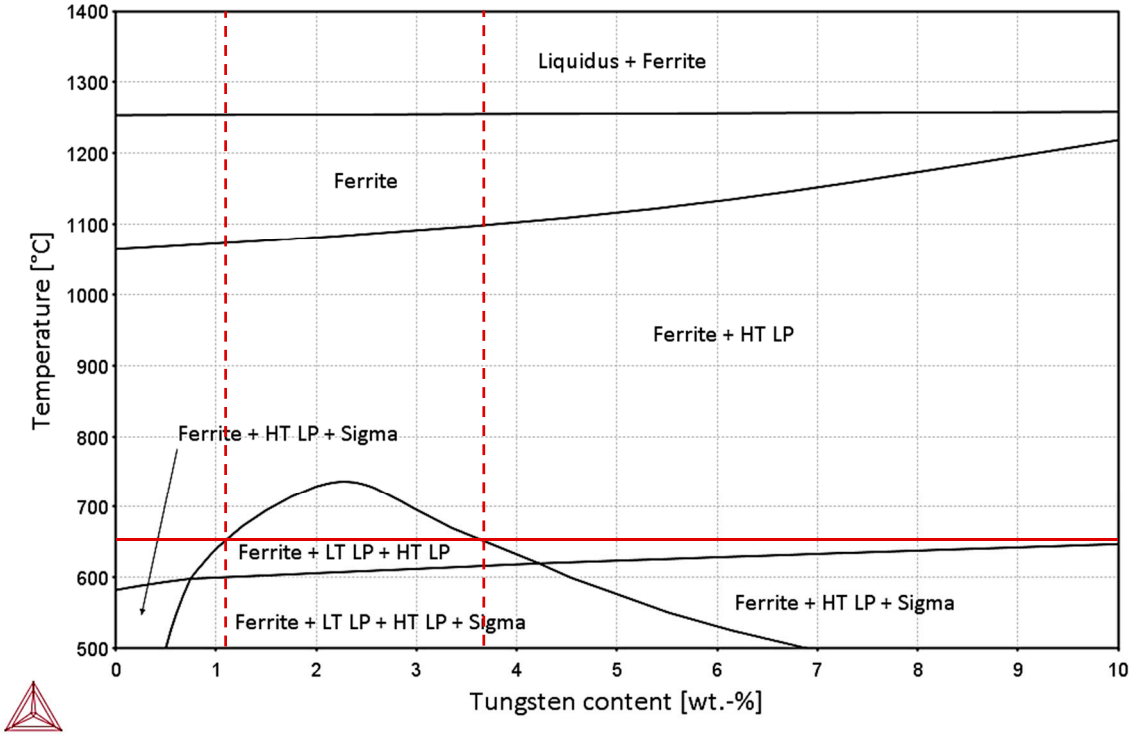


Figure 3. Results of thermodynamic equilibrium calculations of phase diagram (LT LP—Low Temperature Laves Phase, HT LP—High Temperature Laves Phase) as a function of temperature and tungsten content (ThermoCalc®, database TCFE8, nominal chemical composition of 17 wt. % Cr, 0.2 wt. % Mn, 0.25 wt. % Si, and 1 wt. % Nb).

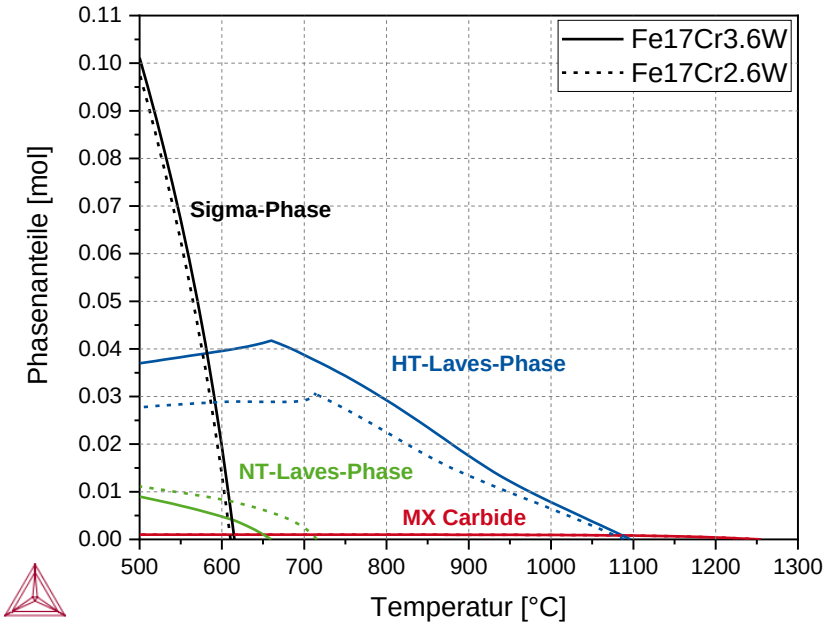


Figure 4. Results of thermodynamic equilibrium calculations of phase amount in tested alloys Fe17Cr with the tungsten content of 2.6 or 3.6 wt. %, respectively (ThermoCalc®, database TCFE8).

A maximum phase fraction of both the strengthening HT and precipitation-promoting LT Laves phases, respectively, was aimed for. For this reason, the effect of tungsten on the phase fraction of the Laves phase was also simulated. Figure 5 shows the simulated phase fraction as a function of tungsten content at 650 °C. Increasing tungsten content promotes the HT and suppresses the LT Laves

phase with an intersection at 1.8 wt. %. Through this additional simulation, a further restriction of the relevant content interval 1.8–3.7 wt. % was achieved. Based on the alloy design, two model alloys, Fe17Cr2.6W and Fe17Cr.3.6W, with varying tungsten content (see the chemical composition in Table 1), were manufactured. The Figure 4 calculation corresponds with the nominal chemical compositions in wt. %: 17 Cr, 0.2 Mn, 0.25 Si, 1 Nb 2.6, and 3.6 W of the model alloys.

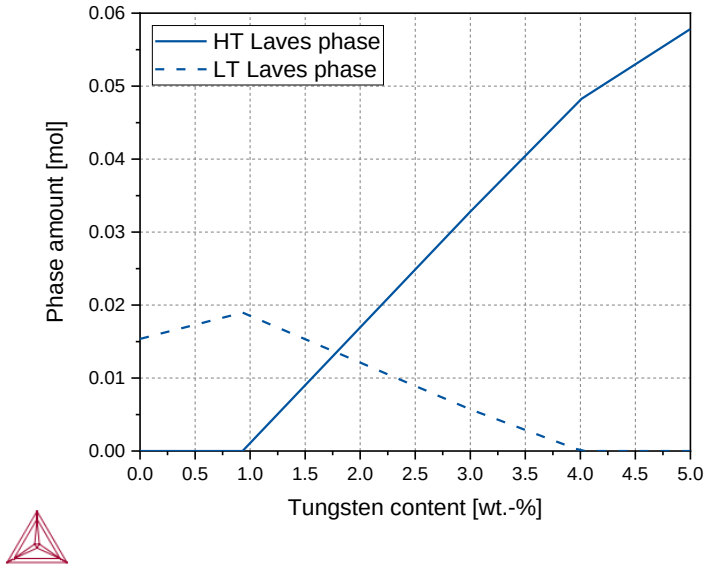


Figure 5. Results of thermodynamic equilibrium calculations of Laves phase amount as a function of tungsten content at 650 °C (ThermoCalc®, database TCFE8).

Table 1. Chemical composition in wt. % of the manufactured model alloys Fe17Cr2.6W and Fe17Cr3.6W.

Model Alloy	C	Si	Mn	Cr	Nb	W
Fe17Cr2.6W	0.0021	0.25	0.19	17.1	0.99	2.6
Fe17Cr3.6W	0.0043	0.25	0.21	17.1	1.01	3.6

Based on the inaccuracy of the recent thermodynamic and kinetic modelling databases, mc_fe_v2.059 and mc_fe_v2.011, respectively, in predicting the precipitation of the multi-componential Laves phase from a ferritic matrix, model calculations of thermomechanically induced precipitation using MatCalc® did not correspond with the observed precipitation behavior during the experimental testing.

3.2. Effect of Tungsten Addition on Laves Phase Precipitation

The effect of tungsten content on the precipitation behavior during thermomechanically induced precipitation was investigated with the alloys Fe17Cr2.6W and Fe17Cr3.6W. An optimized thermomechanical process route with a deformation temperature of 800 °C, a deformation grade of 0.5, and isothermal tempering at the deformation temperature after a forging process of 60 s was chosen. Representative SEM-BSE micrographs of Laves phase evolution are shown in Figure 6. The SEM micrographs show the microstructure states of model alloys achieved with the mentioned constant forging parameters and depict the perpendicular view of the longitudinal cross-section of the deformed central areas of the TTS samples. The new developed process induces a very fine and homogeneous dispersed precipitation structure of the Laves phase. The created rectangular precipitates appear in a linear arrangement form. Particle-free zones along the grain boundaries reach an average width of 630 nm for Fe17Cr2.6W and 825 nm for Fe17Cr3.6W, respectively. Higher tungsten content in the Fe17Cr3.6W model alloy obviously results in the precipitation of slightly larger particles. Due to the higher number of tungsten atoms available in the matrix, the precipitates' growth is promoted.

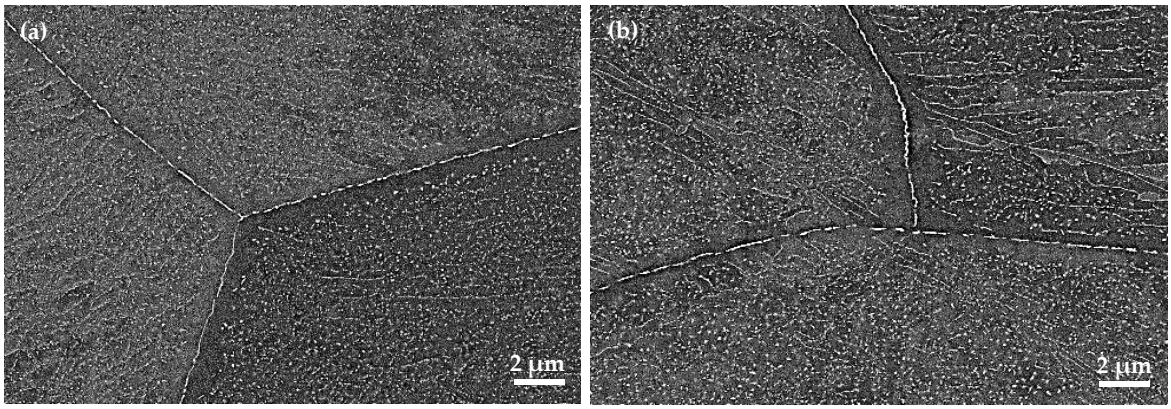


Figure 6. Representative SEM-BSE micrographs of thermomechanically induced Laves phase evolution of model alloys (**a**) Fe17Cr2.6W and (**b**) Fe17Cr3.6W created by deformation at 800 °C, deformation grade of 0.5, and isothermal tempering after the deformation at 800 °C for 60 s.

The high-tungsten model alloy Fe17Cr3.6W with a tungsten content of 3.6 wt. % exhibits an approximately 5% higher strengthening effect in comparison to the low-tungsten model alloy Fe17Cr2.6W with 2.6 wt. % of tungsten (see Figure 7). In other words, increasing the tungsten content results in the precipitation of bigger Laves phase particles (Figure 7a) in a more significant phase fraction (Figure 7b) and enables the reaching of a higher ultimate tensile strength and yield strength (Figure 7c). Due to the higher availability of the dissolved tungsten in the ferritic matrix, the diffusion-conditioned precipitation process is accelerated. Therefore, a faster nucleation and growth of the Laves phase particles are expected. In general, alloying tungsten leads to a more effective solid solution strengthening and supports the Laves phase precipitation. Additionally, tungsten is the main formation element of the stable strengthening HT Laves phase; it promotes the precipitation process and stabilizes the precipitated particles. Corresponding to the results, a 1 wt. % increase in tungsten content results in the precipitation of slightly bigger (approximately 10 nm) particles with a 25% higher phase fraction. The favorable combination of solid solution and precipitation strengthening of the high tungsten model alloy Fe17Cr3.6W enables the reaching of a higher ultimate tensile stress (UTS) of 712 MPa in comparison to the model alloy Fe17Cr2.6W, which results in an UTS of only 683 MPa. The higher strengthening effect is also evident through the increasing of the yield strength value from 412 MPa in the Fe17Cr2.6W alloy to 434 MPa in the Fe17Cr3.6W alloy.

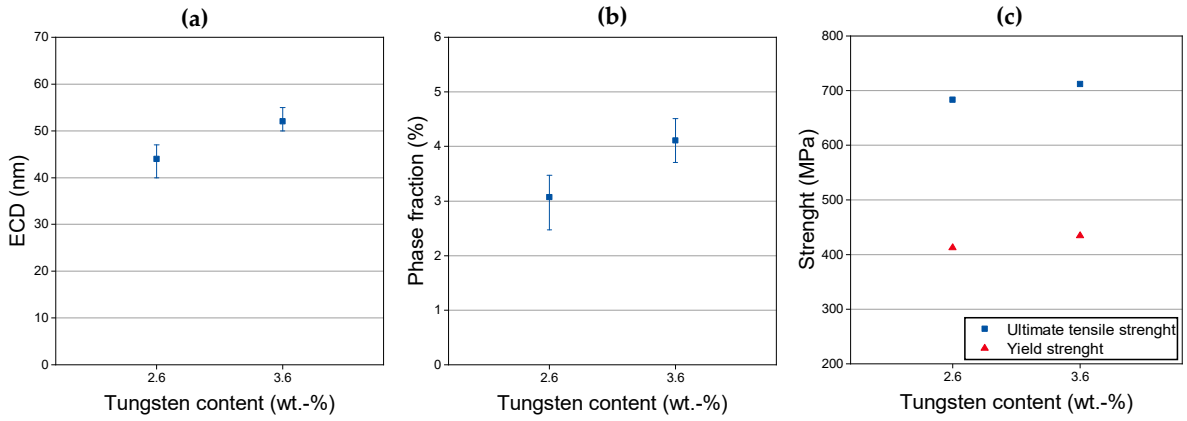


Figure 7. Results of the quantitative particle analysis: (**a**) particle size equivalent circle diameter (ECD), (**b**) phase fraction, and (**c**) ultimate tensile strength and yield strength of model alloys Fe17Cr2.6W and Fe17Cr3.6W.

Due to the higher diffusivity of niobium atoms in the ferritic matrix as compared to tungsten, an early precipitation of the unstable niobium-rich LT Laves phase was observed. Generally, this is attributed to better thermodynamic conditions for nucleation and further growth [23]. However, during ongoing heat treatment, a diffusion flux is created and the LT Laves phase starts to decompose. This continued process of tungsten enrichment during isothermal annealing has been already observed and reported in [23–25]. The higher availability of the tungsten atoms with a slow diffusivity in the ferritic matrix reduces the diffusion distance for the atoms to reach the precipitates. Laves phase precipitation during thermomechanical treatment occurs in this class of steels immediately. Therefore, a noticeable tungsten enrichment of the Laves phase precipitates was expected. A comparison of the chemical composition of the precipitated particles is shown in Figure 8 based on the SEM-EDX analysis. Regarding the EDX-tested area and the size of the analyzed fine particles, the estimated chemical composition does not correspond to the exact composition of the Laves phase precipitates, because the surrounding ferritic matrix influences the results. However, the analysis is sufficient for the investigation of the trend in the developing chemical composition of the precipitates. Additionally, the simulated chemical composition of the unstable LT and stable HT Laves phases are given. The tungsten enrichment of the precipitated Laves phase particles in the high tungsten alloy at the expense of niobium and iron content can be observed. A tungsten content of 11.9 wt. % in Fe17Cr2.6W and 18.8 wt. % in Fe17Cr3.6W, respectively, has been reached. In comparison to the simulated chemical composition, the stable content of tungsten corresponds to 44.5 wt. %. Consequently, a stable state of the HT Laves phase has not been achieved by thermomechanical treatment, and therefore, further tungsten enrichment of the precipitates can be expected during application at operating temperature, as reported in [24].

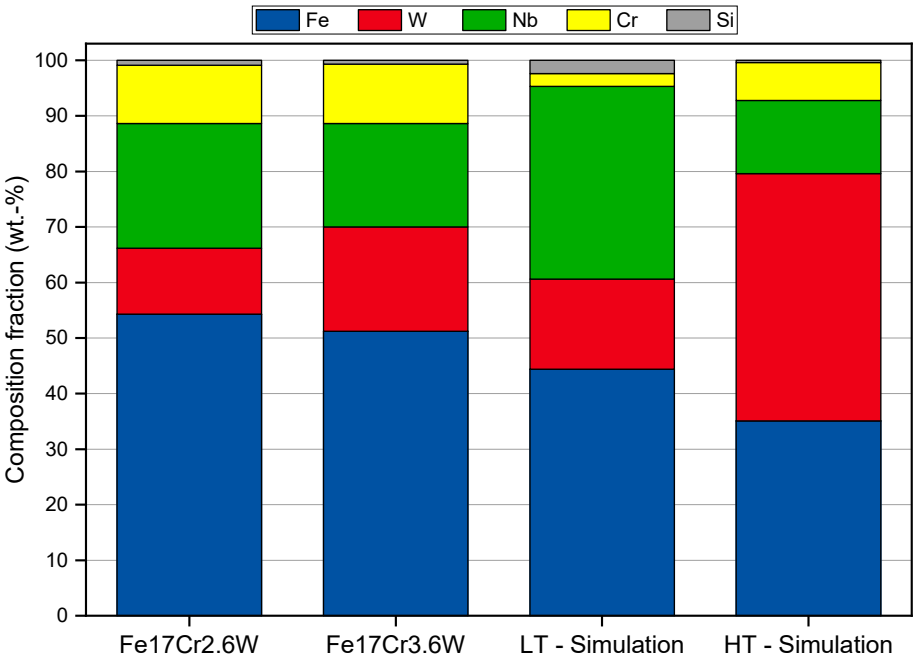


Figure 8. Chemical composition in wt. % of precipitated Laves phase particles in model alloys Fe17Cr2.6W and Fe17Cr3.6W in comparison to the simulated composition of the unstable LT and the stable HT Laves phase (ThermoCalc®, database TCFE8, nominal chemical composition).

3.3. Tensile Properties

The mechanical properties of the Laves phase-strengthened model alloys were determined using small-scale tensile tests performed on sub-sized tensile test specimens, taken from TTS-deformed samples. The strengthening effect of thermomechanically induced precipitation manifests itself in the stress-strain diagram in Figure 9, compared to a particle-free state without deformation. Due to

precipitation strengthening, solid solution strengthening, and strain hardening, a significant level of work hardening was obtained. The progress achieved corresponds to the presence of the homogeneous, finely dispersed Laves phase precipitation. The model alloy Fe17Cr3.6W exhibited a yield strength of 434 MPa and an ultimate tensile strength of 712 MPa. Compared to the undeformed, particle-free state, a progress in strength of approximately 200 MPa can be observed. The alloy Fe17Cr2.6W provides slightly lower values: the yield strength amounted to 412 MPa and the ultimate tensile strength to 683 MPa. The lower phase fraction of the Laves phase in the alloy Fe17Cr2.6W explains the decrease of approximately 30 MPa in strength values.

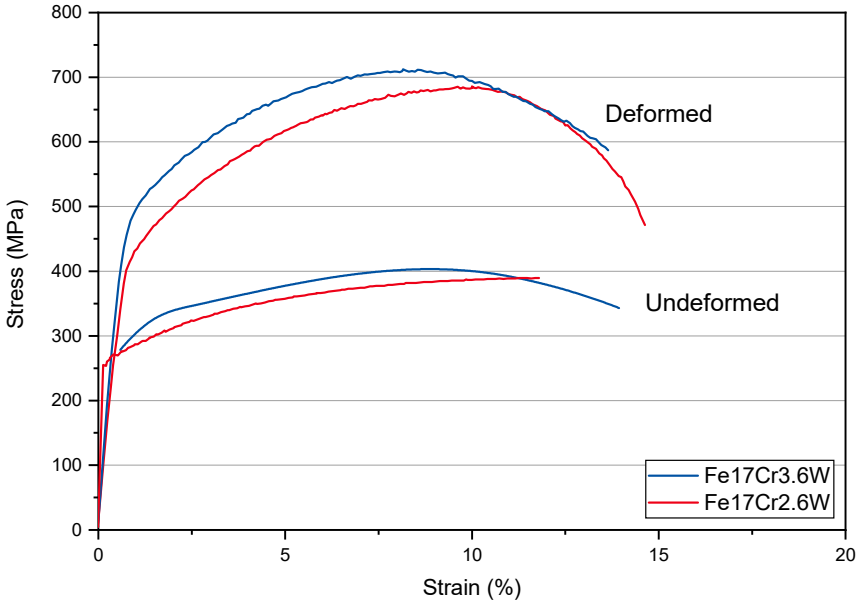


Figure 9. Tensile test results of model alloys Fe17Cr2.6W and Fe17Cr3.6W after the newly developed thermomechanical processing chain in comparison to an undeformed, precipitate-free state.

4. Conclusions

The impact of tungsten on Laves phase precipitation during thermomechanical treatment and on the corresponding strengthening effect in two newly designed fully ferritic model alloys was investigated. The thermomechanical treatments were performed using a thermomechanical treatment simulator (TTS). The investigations of the strengthening effect were performed at ambient temperature. Due to the aim of high-temperature application, the presented results should serve as a base for pursuing the high temperature characterization and further development of this class of steels. The following conclusions can be drawn:

- A fine and homogeneous thermomechanically induced precipitation of the Laves phase in fully ferritic steels is possible and can be controlled by the selection of the deformation parameters. The targeted and fast precipitation within a few minutes during thermomechanical treatment could replace the conventional two-step tempering treatment to precipitate the Laves phase, which takes several hours. As a result, the integrated thermomechanical process opens up a new, more effective, and more economical processing route for high-performance ferritic (HiperFer) stainless steels.
- Tungsten, as the main Laves phase-forming element, is necessary for the desired Laves phase precipitation. In both investigated model alloys with respective tungsten contents of 2.6 wt. % (Fe17Cr2.6W) and 3.6 wt. % (Fe17Cr3.6W), the precipitation of the fine and homogeneous dispersed strengthening Laves phase was achieved. Corresponding to the precipitation strengthening, an increase in yield and ultimate tensile strength of approximately 200 MPa was achieved in comparison to the particle-free, undeformed state. The 1 wt. % higher tungsten content in the

Fe17Cr3.6W alloy results in approximately 30 MPa higher strength values caused by the higher phase fraction of the Laves phase.

- The amount of expensive tungsten is directly related to the total production costs of the alloy. Corresponding to the results, 2.6 wt. % of tungsten is sufficiently beneficial for the desired strengthening effect at ambient temperature. Moreover, a further increase to 3.6 wt.% did not cause significant progress in yield strength or in ultimate tensile strength.

Author Contributions: Conceptualization, J.P. and W.B.; methodology, B.K. and W.B.; investigation, J.P. and X.F.; data curation, J.P. and X.F.; writing—original draft preparation, J.P.; writing—review and editing, B.K., W.B. and U.K.; visualization, J.P.; supervision, W.B. and U.K.; project administration, J.P., W.B. and B.K. All authors have read and agreed to the published version of the manuscript.

Funding: This research received no external funding.

Acknowledgments: The investigations were financially supported by Deutsche Forschungsgemeinschaft (DFG). The authors gratefully acknowledge the support of the staff at the Steel Institute IEHK at RWTH Aachen University and at the Institute of Energy and Climate Research (IEK), Microstructure and Properties of Materials (IEK-2), Forschungszentrum Jülich GmbH in performing the deformation experiments, microstructural investigations and mechanical tests.

Conflicts of Interest: The authors declare no conflict of interest.

References

1. Zurek:, J.; Debruycker, E.; Huymans, S.; Quadakkers, W.J. Steam Oxidation of 9–12% Cr Steels: Critical Evaluation and Implications for Practical Applikation. In Proceedings of the 9th Liége Conference on Materials for Advanced Power Engineering, Liége, Belgium, 27–29 Septemper 2010; pp. 1182–1190.
2. Quadakkers, W.J.; Ennis, P.J.; Zurek, J.; Michalik, M. Steam Oxidation of Ferritic Steels—Laboratory Test Kinetic Data. *Mater. High Temp.* **2004**, *22*, 37–47.
3. Essuman, E.; Meier, G.H.; Zurek, J.; Hänsel, M.; Singheiser, L.; Quadakkers, W.J. Enhanced internal oxidation as trigger for breakaway oxidation of Fe–Cr alloys in gases containing water vapor. *Scr. Mater.* **2007**, *57*, 845–848. [CrossRef]
4. Viswanathan, R.; Bakker, W. Materials for Ultrasupercritical Coal Power Plants-Boiler Materials: Part 1. *J. Mater. Eng. Perform.* **2001**, *10*, 81–95. [CrossRef]
5. Cottis, B.; Graham, M.; Lindsay, R.; Lyon, S.; Richardson, T.; Scantlebury, D.; Scott, H. *Shreir's Corrosion*; Elsevier: Amsterdam, The Netherlands, 2010; Volume 1, pp. 407–456.
6. Mayer, K.H. *Statusreport: Werkstoffentwicklung zur Effizienzsteigerung von fossilen Kraftwerken*; Stahlinstitut VDEh: Düsseldorf, Germany, 2006.
7. Danielsen, H.K.; Hald, J. Behaviour of Z phase in 9–12% Cr steels. *Energy Mater.* **2006**, *1*, 49–57. [CrossRef]
8. Danielsen, H.K.; Hald, J. Influence of Z phase on long-term creep stability of martensitic 9 to 12% Cr-steels. *VGB PowerTech* **2009**, *5*, 68–73.
9. Knežević, V.; Balun, J.; Sauthoff, G.; Inden, G.; Schneider, A. Design of martensitic/ferritic heat-resistant steels for application at 650 °C with supporting thermodynamic modelling. *Mater. Sci. Eng. A* **2008**, *477*, 334–343. [CrossRef]
10. Hald, J.; Korcakova, L. Precipitate stability in creep resistant ferritic steels. In Proceedings of the MPA-NIMS-Workshop–Modern 9–12% Cr-Steels for Power Plant Application, Stuttgart, Germany, 10–11 October 2002.
11. Danielsen, H.K. Precipitation process of Z phase in 9–12%Cr steels. In Proceedings of the 7th International Conference on Advances in Materials Technology for Fossil Power Plants, Waikoloa, HI, USA, 22–25 October 2013; pp. 1104–1116.
12. Kern, T.; Mayer, K.H.; Donth, B.; Zeiler, G.; Digianfrancesco, A. The European Efforts in Development of New High Temperature Rotor Materials–COST 536. In Proceedings of the 9th Liége Conference on Materials for Advanced Power Engineering, Liége, Belgium, 27–29 Septemper 2010; pp. 27–36.
13. Scarlin, B.; Kern, T.U.; Staubli, M. The European efforts in matererial development for 650 °C USC power plants–COST 522. In Proceedings of the 4th International Conference on Advances in Materials Technology for Fossil Power Plants, Hilton Head Island, SC, USA, 25–28 October 2004; pp. 80–99.

14. Kotecki, D.J.; Siewert, T.A. WRC-1992 constitution diagram for stainless steel weld metals: A modification of the WRC-1988 diagram. *Weld. J.* **1992**, *71*, 171–178.
15. Toda, Y.; Tohyama, H.; Kushima, H.; Kimura, K.; Abe, F. Influence of Chemical Composition and Heat Treatment Condition on Impact Toughness of 15Cr Ferritic Creep Resistant Steel. *JSME Int. J. Ser. A* **2005**, *48*, 125–131. [CrossRef]
16. Toda, Y.; Seki, K.; Kimura, K.; Abe, F. Effects of W and Co on Long-term Creep Strength of Precipitation Strengthened 15Cr Ferritic Heat Resistant Steels. *ISIJ Int.* **2003**, *43*, 112–118. [CrossRef]
17. Froitzheim, J.; Meier, G.H.; Niewolak, L.; Ennis, P.; Hattendorf, H.; Singheiser, L.; Quadakkers, W.J. Development of high strength ferritic steel for interconnect application in SOFCs. *J. Power Sour.* **2008**, *178*, 163–173. [CrossRef]
18. Kuhn, B.; Jimenez, C.A.; Niewolak, L.; Hüttel, T.; Beck, T.; Hattendorf, H.; Singheiser, L.; Quadakkers, W.J. Effects of Laves Phase Strengthening on the mechanical Properties of High Cr Ferritic Steels for Solid Oxide Fuell Cell Interconnect Application. *Mater. Sci. Eng. A* **2011**, *528*, 5888–5899. [CrossRef]
19. Kuhn, B.; Talik, M.; Niewolak, L.; Zurek, J.; Hattendorf, H.; Ennis, P.; Quadakkers, W.J.; Beck, T.; Singheiser, L. Development of high chromium ferritic steels strengthened by intermetallic phases. *Mater. Sci. Eng. A* **2014**, *594*, 372–380. [CrossRef]
20. Kuhn, B.; Talik, M.; Fischer, T.; Fan, X.; Yamamoto, Y.; Barrilao, J.L. Science and Technology of High Performance Ferritic (HiperFer) Stainless Steels. *Metals* **2020**, *10*, 463. [CrossRef]
21. Lukas, H.L.; Fries, S.G.; Sundman, B. *Computational Thermodynamics: The CALPHAD Method*; Cambridge University Press: Cambridge, UK, 2007.
22. Thermo-Calc Software. *Thermo-Calc–User's Guide*; Thermo-Calc Software: Stockholm, Sweden, 2016.
23. Barrilao, J.L.; Kuhn, B.; Wessel, E.; Talík, M. Microstructure of intermetallic particle strengthened high-chromium fully ferritic steels. *Mater. Sci. Technol.* **2016**, *33*, 1056–1064. [CrossRef]
24. Lopez Barrilao, J.K. Microstructure Evolution of Laves Phase Strengthened Ferritic Steels for High Temperature Application. Ph.D. Thesis, RWTH Aachen University-FZ Jülich, Aachen, Germany, 2016.
25. Barrilao, J.L.; Kuhn, B.; Wessel, E. Identification, size classification and evolution of Laves phase precipitates in high chromium, fully ferritic steels. *Micron* **2017**, *101*, 221–231. [CrossRef] [PubMed]
26. Kuhn, B.; Talík, M.; Lopez Barrilao, J.; Singheiser, L.; Yamamoto, Y. Development Status of High Performance Ferritic (HiperFer) Steels. In Proceedings of the 8th International Conference on Advances in Materials Technology for Fossil Power Plants, Algarve, Portugal, 10–14 October 2016.
27. Kato, Y.; Ito, M.; Kato, Y.; Furukimi, O. Effect of Si on Precipitation Behaviour of Nb-Laves Phase and Amount of NB in Solid Solution at Elevated Temperature in High Purity 17%Cr-0.5%Nb Steels. *Mater. Trans.* **2010**, *51*, 1531–1535. [CrossRef]
28. Aghajani, A.; Richter, F.; Somsen, C.; Fries, S.; Steinbach, I.; Eggeler, G. On the formation and growth of Mo-rich Laves phase particles during long-term creep of a 12% chromium tempered martensite ferritic steel. *Scr. Mater.* **2009**, *61*, 1068–1071. [CrossRef]
29. Kuhn, B.; Talík, M.; Li, C.; Zurek, J.; Quadakkers, W.J.; Beck, T.; Singheiser, L. Development of Creep- and Corrosion-Resistance Steels for Future Steam Power Plants. In Proceedings of the International VDI Conference on "Alloys in Power Plant Technology", Berlin, Germany, 12–13 June 2012.
30. Isik, M.; Kostka, A.; Eggeler, G. On the nucleation of Laves phase particles during high-temperature exposure and creep of tempered martensite ferritic steels. *Acta Mater.* **2014**, *81*, 230–240. [CrossRef]
31. Nabiran, N.; Klein, S.; Weber, S.; Theisen, W. Evolution of the Laves Phase in Ferritic Heat-Resistant Steels During Long-term Annealing and its Influence on the High-Temperature Strength. *Metall. Mater. Trans. A* **2014**, *46*, 102–114. [CrossRef]
32. Talík, M. Influence of Initial Thermomechanical Treatment on High Temperature Properties of Laves Phase Strengthened Ferritic Steels. Ph.D. Thesis, RWTH Aachen University-FZ Jülich, Aachen, Germany, 2016.



© 2020 by the authors. Licensee MDPI, Basel, Switzerland. This article is an open access article distributed under the terms and conditions of the Creative Commons Attribution (CC BY) license (http://creativecommons.org/licenses/by/4.0/).